ELSEVIER

Journal of Nuclear Materials 317 (2003) 195–203

journal of nuclear materials

www.elsevier.com/locate/jnucmat

Permeation of hydrogen through tantalum: influence of surface effects

A. Pisarev [a,*], K. Miyasaka [b], T. Tanabe [b]

[a] Department of Physics, Moscow Engineering and Physics Institute, Kashirskoe shosse, Moscow 115409, Russia
[b] Center for Integrated Researches in Science and Engineering, Nagoya University, Nagoya 464-8603, Japan

Received 20 September 2002; accepted 25 January 2003

Abstract

Gas driven permeation of hydrogen through Ta has been investigated at 900 K and $p = 50$–5000 Pa. The permeation rate as a function of time has a peaked shape: after initial rise, it decreases for several hours, remaining approximately proportional to the gas pressure, which is the feature of the surface limited regime (SLR). Computations using an SLR model were performed. It was concluded that the Ta membrane becomes asymmetric due to the contamination of the inlet surface. The solubility $S = (9.3 \pm 3.0) \times 10^{18}$ H cm^{-3} Pa$^{-1/2}$ is in good agreement with data available from literature. The recombination and absorption coefficients K and K_a have been obtained in the ranges $K = (6\text{–}500) \times 10^{-26}$ at^{-1} cm^4 s^{-1} and $K_a = (3\text{–}200) \times 10^{12}$ at cm^{-2} s^{-1} Pa^{-1}, respectively. The values of K_a are very low. It has been concluded that long permeation experiments need special measures for purification of the working gas.

1. Introduction

Permeation through metals with a negative heat of solution (V, Nb, Ta) is strongly different from permeation through metals with a positive heat of solution. The potential energy levels of hydrogen atoms in metals of the former group are below the energies of these atoms in the hydrogen gas molecules. In this case, hydrogen is 'trapped' between surface potential walls, and surface effects restrict its permeation [1–3]. Therefore it is invalid to use the diffusion-limited approach and it is problematic to obtain the diffusion coefficient from permeation experiments with these metals.

The gas driven permeation experiments performed in [3,4] in surface limited regime (SLR) were well described by a simple model based on the suggestions that the distribution of hydrogen in the membrane is uniform and the desorption rate is proportional to the square of the bulk concentration. Solubility and surface rate coefficients can be obtained by applying this model to SLR measurements.

Experiments in SLR are influenced by surface properties, which unpredictably depend on experimental conditions. Several works performed with V and Nb demonstrated that impurity segregation on surfaces of these metals could influence the permeation rate [5–12]. But the experiments were mainly performed with energetic hydrogen particles (ions and atoms).

Analyses of permeation experiments performed in SLR become difficult due to possible asymmetry of the membrane: the inlet and the outlet surface properties are not obligatory identical. More likely that they are different. This may bring an uncertainty in the interpretation of the experimental data.

This work is devoted to analyses of possible effects that can arise in the SLR of gas driven permeation through exothermal metals due to surface contamination in the course of long experimental runs. We will demonstrate for this purpose that the permeation rate gradually decreases for a long time after reaching a 'steady-state' value. The observed decrease of permeation

* Corresponding author. Tel.: +7-095 323 9325; fax: +7-095-324 7024.
E-mail address: pisarev@plasma.mephi.ru (A. Pisarev).

0022-3115/03/$ - see front matter © 2003 Published by Elsevier Science B.V.
doi:10.1016/S0022-3115(03)00079-5

will be analyzed suggesting that the surface can be gradually passivated during long experimental runs. We will analyze the cases of symmetric and asymmetric membranes and discuss the uncertainty of modeling typical for SLR. We will analyze, which surface is most probably responsible for decrease of permeation, and estimate the values of the solubility, recombination coefficient, and absorption coefficient.

2. Experiments

The experiments were performed using the installation for the permeation measurements described in details in [4]. It is mainly made of stainless steel and has the base pressure of less than 10^{-7} Pa. A tantalum specimen disk separates the vacuum chamber into two parts.

Hydrogen gas was admitted into one part (the inlet side), permeated through the membrane, and is measured in another part (the outlet side). Experiments were made at three gas pressures of 53, 530, and 5300 Pa. Research grade (99.999%) hydrogen was used. To avoid hydrogen contamination during the experiment, the hydrogen gas was continuously supplied to and simultaneously pumped out of the inlet chamber. The gas pressure was controlled and kept constant during the experiment. The hydrogen pressure was monitored by a capacitance manometer on the inlet side, and by an ionization gauge on the outlet side. The ionization gauge working in hydrogen was calibrated with respect to nitrogen, and the relative sensitivity was found to be 0.4.

The outlet side was continuously pumped out with the pumping speed of about 10^{-1} m^3 s^{-1}. In this case, the rise of the gas pressure in the outlet chamber was directly proportional to the gas release rate into the chamber. Therefore, the hydrogen permeation rate was just the signal of the hydrogen partial pressure read from a calibrated quadrupole mass spectrometer.

The Ta membrane specimen with the nominal purity of 99.99% was fixed on a stainless steel sample holder using metal gaskets without any vacuum leak. The thickness and surface area of the specimen were 0.05 mm and 1.8 cm^2, respectively. It was mechanically polished with 0.3 μm alumina powder, rinsed in acetone, and annealed at 1200 K for 1 h in vacuum before the measurements. A molybdenum heater surrounding the specimen holder heated the sample, and the temperature, which was measured by a thermocouple, was kept at (900 ± 5) K.

It was observed in the experiment that the permeation rate increased to some maximum value after applying the gas pressure, but then slowly decreased if permeation was measured for a long time. The time dependences of the experimental permeation rates are shown in Fig. 1. One can see three stages in each permeation run: the initial increase to a maximum value (stage 1), subsequent slow decrease (stage 2), and fast decay after removing gas from the inlet side (stage 3). Two series of experiments with an interval of about a month were performed. The numbers near the curves hereafter are the days of the year and the number of the series (in brackets).

The effect of permeation decrease on the second stage of the measurements has several qualitative explanations. The first one is that the surface of the sample can become contaminated during the permeation run. The second one is that the diffusion coefficient decreases if the concentration of hydrogen increases. The third one

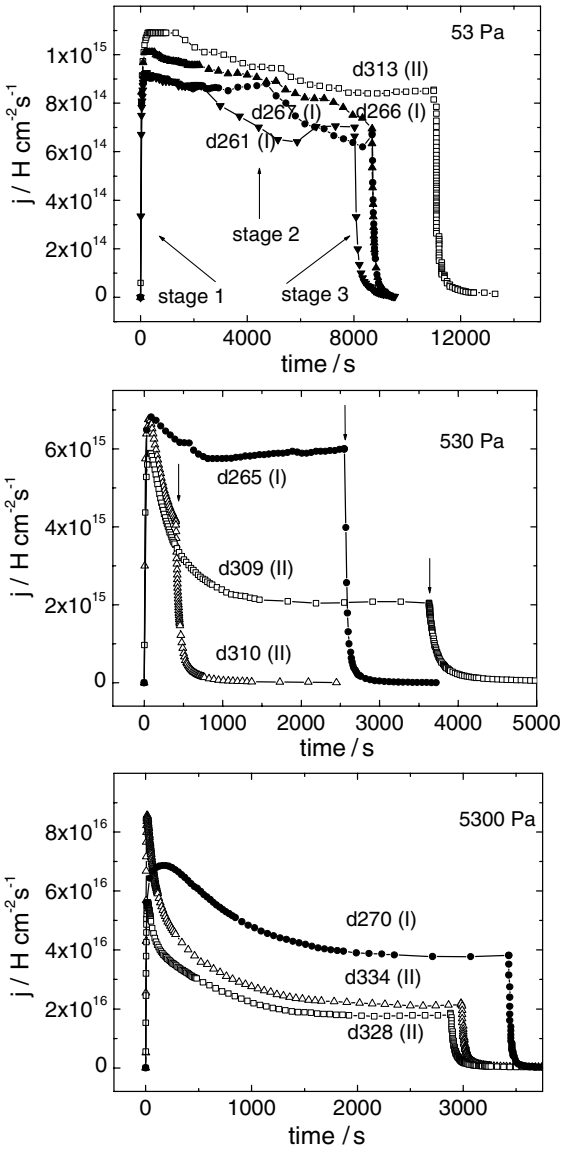

Fig. 1. Permeation experiments.

is that accumulation of hydrogen can provoke formation of hydrides, which suppress diffusion.

The basic properties of H-metal systems are summarized in two books of reviews [13]. The diffusivity of hydrogen in Ta is very fast. At 900 K it is about 1×10^{-4} $cm^2\,s^{-1}$, so it takes a second to diffuse to the distance of 0.1 mm. This confirms the validity of the approach of the uniform concentration distribution accepted in SLR modeling. Estimations of the concentration from the solubility show that it does not exceed a few atomic percent in these experiments. In this case neither decrease of the diffusivity nor formation of hydrides can be expected.

The decision about the limiting stage of permeation is often made basing on the analyses of the pressure dependence of the steady-state permeation rate. There is no exact steady-state permeation in the experimental plots of Fig. 1, but one may suggest that permeation is in a 'quasi-steady-state' regime in the region of the maximum and after the maximum. Fig. 2 shows the pressure dependences of the permeation rates in the maximum and at the end of the second stage. One can see that they are well described by simple linear lines $j_{max} = 1.5 \times 10^{13} p$ and $j_{fin} = 0.9 \times 10^{13} p$. This means that SLR is the case of the experiments from the beginning and to the end of measurements. Strictly speaking, the pressure dependence is better described by the 0.92 power function at the end of the permeation run. Nevertheless, deviation from the linear pressure dependence is small, and this may be considered as an evidence of the SLR. Anyway, $p^{0.5}$ dependence typical for the diffusion-limited regime cannot be applied to the experimental pressure dependences. That is, even if diffusion becomes slower due to some reasons during the experiment, it still does not limit the permeation.

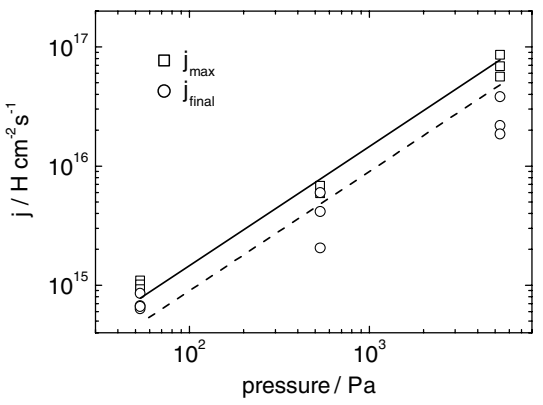

Fig. 2. Pressure dependence of the permeation rate in the maximum of the permeation curve and at the final point of stage 2. Lines are linear pressure dependences drown through the experimental points.

Therefore, we will analyze only the first suggestion about the possible reason of the peaked permeation curve, namely, contamination of the surface during long permeation runs. One must remind that an ultrahigh vacuum system and high-grade purity hydrogen gas were used in the experiment, but nevertheless the surface of Ta could become contaminated.

Passivation of both the inlet and outlet surfaces can lead to a decrease of the permeation rate. It is difficult to predict which surface changes during the experiment. One can only suggest that the conditions on the outlet surface, which is in contact with vacuum, are more stable than the conditions on the inlet surface, which is in contact with gas. Nevertheless, we will analyze both possibilities.

3. Model

The SLR is often characterized by a flat profile with hydrogen uniformly distributed all over the sample bulk. This gives an opportunity of simple modeling of permeation as it was made in [3,4].

The simplest suggestion that can be made is that the recombination coefficients on the inlet and outlet sides are equal to each other (so-called symmetric membrane) and both change during the second stage of the experiment. In this case one may apply the SLR model described in [3] to the first and the third stages of the experimental run using two different values of the recombination coefficient in these stages. Attempts of modeling this situation were not successful. It was possible to adjust either stage 1 or stage 3 but not both. The reason is quite obvious. There are three basic parameters in the model (solubility and recombination coefficients in the stages 1 and 3). But there are at least four parameters characterizing the stages 1 and 3 (absolute values of the permeation fluxes at the end of stage 1 and at the beginning of stage 3 and two characteristic times of these stages). Therefore, the number of model parameters is not enough to characterize both stages together. It may happen that good agreement is obtained for both stages, but this can be only in the case where the membrane is symmetric in the experiment. Therefore the obtained disagreement leads to the conclusion that the membrane is asymmetric, i.e. the inlet and outlet surfaces have different recombination coefficients (K_1 and K_2 respectively).

In the case the recombination coefficients on the two sides of the asymmetric membrane change from some initial values at the beginning of the experiment to some final values at the end of the experiment, the number of fitting parameters increases and can become too large to describe the features of the experimental curves. Therefore, additional suggestions have to be made to reduce the number of fitting parameters. There are four

characteristic parameters describing the first and the third stages of the experiment, therefore we need four free parameters in the model. They are: the solubility and three values left for the recombination coefficients. Therefore, additional suggestions have to be made to reduce the number of free parameters. In application to our experiment, they are as follows. Firstly, the surface recombination coefficients on the inlet side and the outlet side have been taken time-invariable during the first and third stages of the permeation run (let us denote the respective recombination coefficients as initial and final: K_{1i}, K_{2i} and K_{1f}, K_{2f}). Hereafter, all the initial and the final values also mean the values at the beginning and at the end of the second stage of the quasi-steady-state permeation, respectively. Secondly, during the stage of slow decrease of the permeation rate (second stage of the permeation run) only one of the coefficients (either K_1 or K_2) have been allowed to decrease, while another (either K_2 or K_1) has been kept invariable. The absorption flux i_a depends on the inlet surface characteristics. Therefore, the absorption fluxes at the beginning and at the end of stage 2, which we denote as the initial and the final values i_{ai} and i_{af} can be either different (if we model the variant where the inlet side changes) or equal (if we model the variant where the outlet side changes).

Suggesting that the concentration is depth-independent, the concentration build-up $c_1(t)$ during the first stage ($t = 0 - t_m$), where t_m is the time corresponding to the maximum value of permeation, can be described by the simple differential equation (1) with the initial condition (2) similar to the writing made in [3]:

$$dc_1/dt = (i_{ai} - (K_{1i} + K_{2i})c_1^2)L^{-1}, \tag{1}$$

$$c_1(t = 0) = 0. \tag{2}$$

The concentration $c_3(t)$ during the permeation decay (the third stage, time $t > t_f$) is described by Eq. (3) with the initial condition (4)

$$dc_3/dt = -(K_{1f} + K_{2f})c_3^2L^{-1}, \tag{3}$$

$$c_3(t = t_f) = c_f. \tag{4}$$

Here the time $t = t_f$ is the final time of the second stage, and at the same time it is the initial time of the third stage. Respectively c_f is the final concentration of the second stage and the initial concentration of the third stage.

Additionally to Eqs. (1)–(4), one can write two more equations linking the parameters of the model. One of them is based on the fundamental relationship between the recombination coefficient K, absorption coefficient K_a and solubility S, which can be obtained from consideration of the balance of the absorption (i_a) and re-emission (j_r) fluxes in the sample totally embedded in the gas:

$$i_a = 2K_a p = j_r = Ku_S^2 = KS^2 p, \tag{5}$$

where $u_S = Sp^{1/2}$ is the equilibrium (or Sieverts) concentration, which is established in the sample in thermodynamic equilibrium with gas according to the Sieverts law. The values of K_a and K in Eq. (5) correspond to the surface in contact with gas. Therefore, this equation must be applied to the inlet side of the membrane. This gives

$$i_{ai}/i_{af} = K_{1i}/K_{1f}. \tag{6}$$

Another equation linking the parameters is connected with the restrictions that only one of the sides changes during the stage 2, that is: either $K_1 = \text{var}$, $K_2 = \text{const}$ (variant 1) so that

$$K_{2i} = K_{2f} \tag{7a}$$

or $K_1 = \text{const}$, $K_2 = \text{var}$ (variant 2) so that

$$K_{1i} = K_{1f}. \tag{7b}$$

Solving (either numerically or analytically) six equations ((1)–(4), (6), (7)) and fitting the solution to the experimental data, one can find six parameters K_{1i}, K_{2i}, K_{1f}, K_{2fi}, i_{ai}, i_{af}. The important point of the fitting procedure is the proper choice of guess values to start fitting. These values can be calculated using four characteristic points of the permeation curve: maximum of stage 1 ($t_m = t_i$), beginning of stage 3 (t_f), a point in the beginning of stage 1 characterizing the rate of the permeation increase, and a point of stage 3 characterizing the rate of the permeation decay.

At the point of the maximum one can write two equations:

$$j_i = K_{2i}c_i^2 \tag{8}$$

and

$$i_{ai} = (K_{1i} + K_{2i})c_i^2, \tag{9}$$

where $j_i = j_m$ and $c_i = c_m$ are the permeation rate and concentration in the maximum of the permeation curve.

Similar equations can be written at the point of the end of gas supply t_f.

$$j_f = K_{2f}c_f^2 \tag{10}$$

and

$$i_{af} = (K_{1f} + K_{2f})c_f^2, \tag{11}$$

where j_f and c_f are the permeation rate and concentration at the end of stage 2.

At the very beginning of the stage 1 ('zero' time $t = t_0 \ll t_m$), where the concentration is very low, Eqs.

(1) and (2) give that the concentration increases linearly in time

$$c_0(t_0) = t_0 i_{ai} L^{-1} \tag{12}$$

and the permeation rate ($j = K_2 c^2$) is a parabola

$$j_0(t_0) = (K_{2i} i_{ai}^2 L^{-2}) t_0^2. \tag{13}$$

The values of j_0 and t_0 are supposed to be taken from the experiment, and $j_0(t_0)$ point can be chosen rather arbitrarily.

Solution of the Eqs. (3) and (4) for the stage 3 leads to the following time dependence of the permeation rate decay

$$j_3(t) = K_{2f} c_f^2 [1 + (K_{1f} + K_{2f}) c_f L^{-1} (t - t_f)]^{-2}. \tag{14}$$

From this equation one can find a characteristic decay time. This can also be done rather arbitrarily. For example, it is convenient to use the point, at which the permeation rate j_3 decreases 4 times and becomes equal to $j_f/4$ at the time t_3 which can be found from

$$(K_{1f} + K_{2f}) c_f L^{-1} (t_3 - t_f) = 1. \tag{15}$$

Solving eight equations (6), (7a), (7b), (8)–(11), (13) and (15) together, one can find eight parameters: K_{1i}, K_{2i}, K_{1f}, K_{2f}, c_i, c_f, i_{ai}, i_{af} if the rates j_0, j_i, j_f and times t_0, t_3 are taken from the experimental permeation curve. After this, the increasing and decaying permeation rates can be calculated according to Eqs. (1) and (3). Having in hands the values of the absorption flux i_a and the recombination coefficient on the inlet side K_1 one can calculate the absorption coefficient K_a and the solubility S using Eq. (5).

4. Calculations and discussion

Figs. 3 and 4 show the examples of calculations for the stages 1 and 3. Two variants are considered: in one of them, the recombination coefficient changes on the inlet side during stage 2; in another, on the outlet side. These two variants employ either Eq. (7a) or Eq. (7b), respectively. Calculations for the stage 1, Fig. 3, have given a perfect agreement at the highest pressure of 5300 Pa and a rather good agreement at the lowest pressure of 530 Pa. The case of 53 Pa has given an intermediate agreement and therefore is not shown in Fig. 3. Calculations for the stage 3, Fig. 4, have demonstrated perfect agreement with all the experimental runs at the three pressures. Fig. 4 contains the data only for 530 Pa to demonstrate three experimental decay curves obtained after termination of gas supply at three different moments t_f shown by arrows in Fig. 1.

One must note that the two variants of calculations have given equally good agreement, and one can hardly see any difference between the two respective calculated curves given by solid and dashed lines in Figs. 3 and 4.

This situation seems surprising from the first glance. But the reason is obviously universal. Any set of points

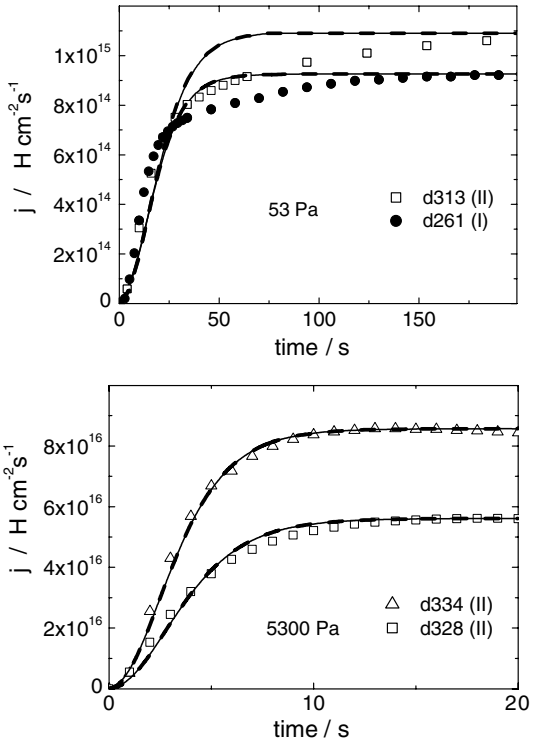

Fig. 3. Permeation during stage 1. Dots are the experiment. Thin solid and thick dashed lines are for two variants of calculations made in the suggestion that the recombination coefficient during stage 2 decreases either on the inlet or on the outlet side, respectively.

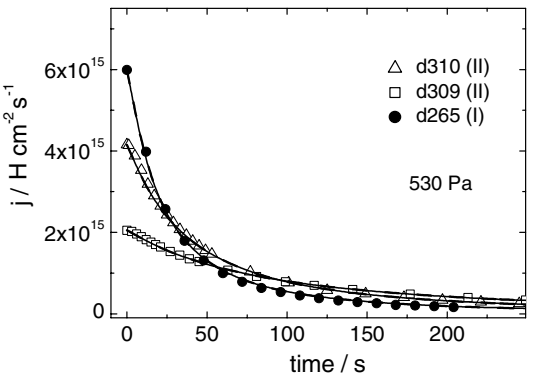

Fig. 4. Example of the permeation decay during stage 3. Dots are the experiment. Solid and dashed lines are two variants of calculations as in Fig. 3.

can be described by several functions; therefore, several models can describe any experimental data set. If a model suits the experiment, this does not mean that the model is correct, this only means that the model is not in conflict with the experiment. Unfortunately, in our case neither of the models is in conflict with the experiment. Therefore, the choice between the models must be made using some additional analyses, which we will try to make below.

One could suggest that the second stage of the experimental run could be of use. Unfortunately, it is useless because the description of this stage needs additional questionable suggestions. For example, one must suggest how the recombination coefficient changes in time.

A judgment about the validity of the model could be made from an analysis of the values of the parameters obtained. Unfortunately, no remarks can be made about the recombination coefficient and the absorption coefficient (connected with the absorption rate) as they can change during the experiment and no information is available from the literature. The concentrations, obtained in both variants of calculations, rise with the gas pressure and do not exceed the reasonable value of 2×10^{21} H/cm^3 (about 3.6 at.%) at the highest pressure of 5300 Pa. So, both variants are satisfactory from the point of view of the concentration values.

The fundamental parameter, which can be used for the analyses, is the solubility, which is well known for Ta. The experiments on permeation have been made several times at every pressure with the interval between measurements ranging from one day to one month to verify the stability of measurements. Solubilities obtained in two variants of calculations are given in Fig. 5 as a function of the day of the experimental campaign and the gas pressure. The average value of the solubility obtained in both variants of calculations is approximately the same (9.3×10^{18} and 8.2×10^{18} H cm^{-3} Pa$^{-1/2}$ in the first and the second variants, respectively). These values are close to the value of 1.45×10^{19} H cm^{-3} Pa$^{-1/2}$ obtained in [14] in a series of extensive researches on the solubility of hydrogen in metals of group V. Though the first variant gives a 'better' value, the difference is not large, and one can consider that both variants give reasonable solubility values.

To make a decision which variant is correct, one can analyze the stability of the fitting parameters during the experimental campaign and the dependence on the gas pressure. One can see from Fig. 5 that the solubility obtained in the first variant of calculations has no distinct tendencies of variation with the time and the pressure used. This is not the case of the second variant: we observe a gradual rise of the solubility during the campaign and its increase with the pressure. The solubility is a fundamental parameter, which must be a constant for a given material at given temperature.

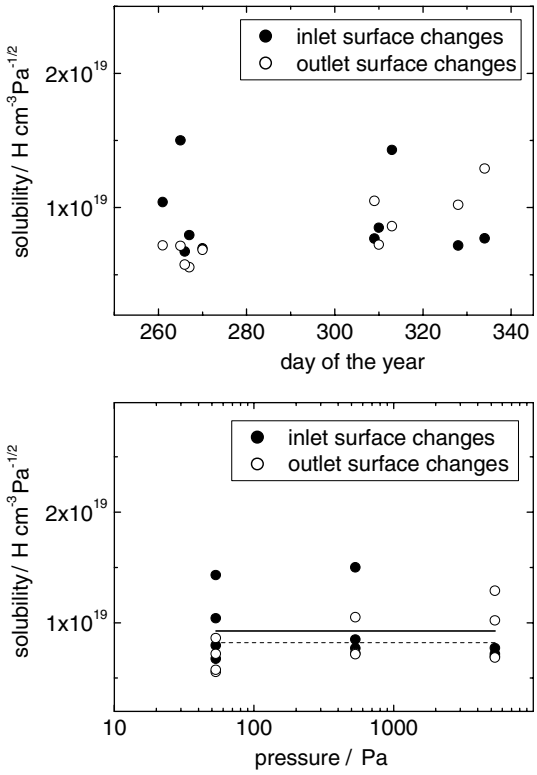

Fig. 5. Variation of the solubility during the experimental campaign and as a function of pressure for two variants of calculations. Solid symbols – the inlet surface changes. Open symbols – the outlet surface changes. Solid and dashed lines – the average values for these two variants of calculations.

Therefore, one can conclude that it is more likely that the first variant is correct, that is the inlet surface characteristics changed during stage 2 of the experimental run. The solubility in this case can be estimated as $(9.3 \pm 3.0) \times 10^{18}$ H cm^{-3} Pa$^{-1/2}$.

The recombination coefficients for Ta are not available from the literature. The recombination coefficients for any metal strongly depend on the surface conditions. Therefore, these permeation measurements have given an opportunity to evaluate the range of possible values of K in one experimental run. These values on the inlet and outlet sides at the beginning and at the end of stage 2 calculated in two variants are shown in Fig. 6 as a function of the pressure. One can see that the range of values of the recombination coefficients is very large. In the first variant of calculations, the recombination coefficient decreases during the second stage approximately by one order of magnitude from the initial value $K_{1i} = (1–5) \times 10^{-24}$ H^{-1} cm^4 s^{-1} to the final value $K_{1f} = (1–6) \times 10^{-25}$ H^{-1} cm^4 s^{-1}, of the same order as the recombination coefficient on the outlet side $K_2 = (0.6–5) \times 10^{-25}$ H^{-1} cm^4 s^{-1}. The second variant of calculations gives a much broader range of the recombination coef-

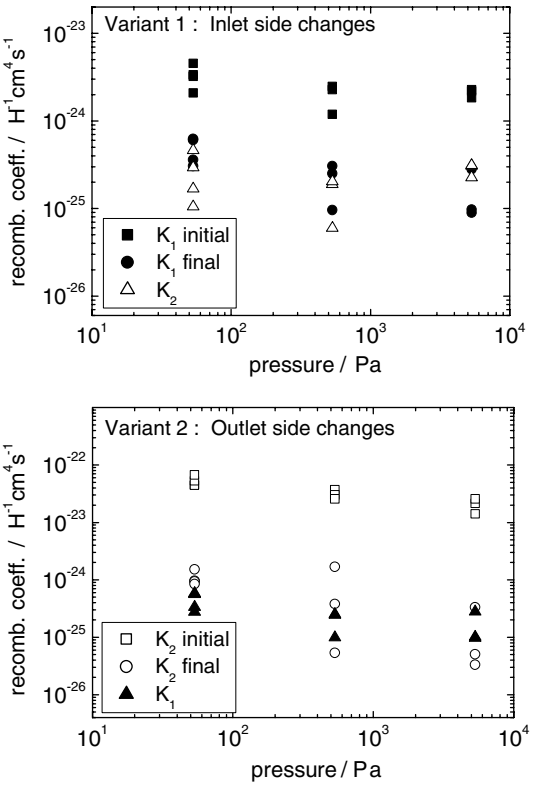

Fig. 6. Variation of the recombination coefficients on the inlet and outlet sides with the gas pressure. Two variants of calculations have been made: suggesting that either inlet or outlet surface changes during stage 2 of the experimental run.

ficient $K_2 = (0.3\text{–}700) \times 10^{-25}$ $\mathrm{H^{-1}\,cm^4\,s^{-1}}$ and similar tendencies of the time and pressure evolutions.

The analysis of the campaign history shows that there is a tendency of decreasing of all the K during the campaign. This means that the surfaces become gradually modified during the long experimental campaign. One can also see from Fig. 6 that the K values slightly decrease with pressure. This could be due to a higher surface contamination at a higher gas pressure.

One must mention that the membrane is strongly asymmetric in the beginning of each experimental run in both variants of calculations; the difference in the recombination coefficients on the inlet and the outlet sides is 1–2 orders of magnitude. This difference becomes much less in the end of the experimental run. Moreover, the asymmetry can even change its direction ($K_1/K_2 - 1$ changes the sign) at the end of the experimental run as it takes place at the highest pressure. One must also mention the principal difference in data obtained in two variants of calculations. The first variant gives a very high initial value of the recombination coefficient on the inlet side, while the second variant gives a very high initial value of the recombination coefficient on the outlet side. This means that the modes of initial permeation are different in these two variants of calculations. If $\gamma = K_2/K_1 \ll 1$, the permeation is limited by recombination of atoms on the outlet side (recombination limited regime, RLR), and this is the case of the first variant of calculations. If $\gamma = K_2/K_1 \gg 1$, the permeation is limited by absorption of hydrogen on the inlet side (absorption limited regime, ALR), and this is the case of the second variant of calculations. These two regimes give different ratios of the permeation flux j to the re-emission flux j_r One can find that only a minor part of absorbed particles permeates through the membrane ($j \ll j_r$) in RLR (the first variant). In the second variant (ALR) we observe $j \gg j_r$; i.e. practically all the absorbed atoms permeate through the membrane.

During stage 2, the situation changes in a way, that the re-emission flux $j_r(t)$ decreases in the first variant and increases in the second variant due to decrease of K_1 and K_2 respectively. In the case of a high pressure, this effect leads even to the change of the mode of permeation as can seen from Fig. 7.

The change of the recombination coefficient during permeation can lead to peculiar effects. For example, interrupting the permeation run in stage 2 at several different moments, as it is shown in Fig. 1 for $p = 530$ Pa, and measuring the permeation decay rates in stage 3, one can observe that the number of particles releasing from the outlet side in stage 3 increases with the duration of stage 2. This could be interpreted as an increase of the concentration in the sample during stage 2. But this is not always correct in the case of the asymmetric membrane having varying recombination coefficients. If the recombination coefficient on the outlet side decreases in time, the concentration in the sample increases. But the situation is different if the recombination coefficient on the inlet side decreases in time: the concentration in the sample in this case decreases due to the decrease of

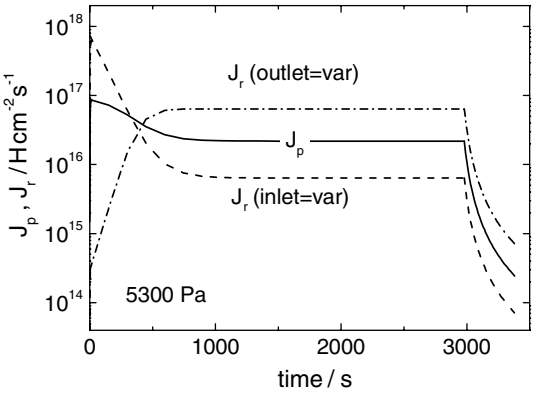

Fig. 7. Typical behavior of the permeation and re-emission rates in two variants of surface changes.

the absorption rate (and this is the case of the first variant). At the same time, the number of particles releasing from the outlet side during stage 3 increases due to the increase of the K_2/K_1 ratio. Measurements of the gas release only into the outlet chamber can mislead in estimations of the number of hydrogen stored in the asymmetric membrane.

The values of the absorption coefficient can be calculated from the recombination coefficient and solubility using Eq. (5): $K_{ai} = (56–214) \times 10^{12}$ H cm^{-2} s^{-1} Pa^{-1} and $K_{af} = (3–34) \times 10^{12}$ H cm^{-2} s^{-1} Pa^{-1} in the first variant and $K_a = (5–10) \times 10^{12}$ H cm^{-2} s^{-1} Pa^{-1} in the second variant. These values are quite low. Indeed, if the flux of particles, which impinge the surface from gas, is calculated from the kinetic theory of gases and the flux of absorbed particles – from Eq. (5), one can find that the probability of absorption is very low: $A_i = (1–5) \times 10^{-5}$ and $A_f = (5–80) \times 10^{-7}$ for the first variant and $A = (1–3) \times 10^{-6}$ for the second variant of calculations. That is, the surface of Ta becomes seriously contaminated in the experiment. This conclusion seems to be important for any metal of the group V, which can be easily contaminated even in a good vacuum by admitting even a pure hydrogen gas. It is important to take care about additional measures for purification of hydrogen gas when working with metals of the group V.

5. Conclusions

The hydrogen gas driven permeation rate through Ta measured at 900 K and at the gas pressures 53, 530, and 5300 Pa has been found to decrease during long (several hours) permeation runs. Three stages of the permeation curve have been measured: (1) initial fast increase after the pressure application, (2) slow and long decrease at the pressure applied, and (3) fast decay after evacuation of the permeation driving gas.

It has been observed that the permeation rate is proportional to the hydrogen pressure during stage 2. This means that the permeation is limited by surface processes, the diffusion model cannot be applied and the diffusivity cannot be extracted, and the permeation decreases due to changes on the membrane surfaces during long permeation runs.

The experimental data have been analyzed by applying the model of the SLR of permeation with the recombination coefficient being a function of time. It has been demonstrated that the first and the third stages of the experiment cannot be fitted together in the suggestion of the symmetric membrane. This means that the Ta membrane becomes asymmetric when used in permeation experiments, that is the surface properties of its sides become different.

It has also been shown that measurements of only the increasing part of the permeation curve cannot give reliable information in the case of the asymmetric membrane because of the excess of freedom in choosing the model parameters.

Modeling of the permeation through the asymmetric membrane has been performed in two variants: (1) the inlet surface contaminates and (2) the outlet surface contaminates. It has been found that both variants give equally a good description of the experiment. The solubilities obtained in these two variants are very close to each other. That is, even measurements of the rise and decay stages together in the case of an asymmetric membrane cannot give an exact answer to the question which side of the membrane is more severely contaminated.

Multiple measurements performed during a long experimental campaign at three gas pressures have demonstrated that the solubility value in the first variant of calculations has no distinct tendencies of variation with the time and the pressure. In the second variant, the solubility rises in time and with the pressure. Therefore, it has been concluded that the inlet surface of Ta becomes contaminated from the hydrogen gas, though it was purified before supplying to the permeation unit. Even the regime of permeation can change from the recombination limited permeation to the absorption limited permeation due to surface effects in the course of a long experiment.

The solubility at 900 K obtained in the first variant of modeling (the inlet side changes during the experiment) is $(9.3 \pm 3.0) \times 10^{18}$ H cm^{-3} Pa$^{-1/2}$, which is in good agreement with data available from the literature. The recombination coefficient on the inlet side in this variant decreases during the experiment approximately by an order of magnitude from the initial value $K_{1i} = (1–5) \times 10^{-24}$ H^{-1} cm^4 s^{-1} to the final value $K_{1f} = (1–6) \times 10^{-25}$ H^{-1} cm^4 s^{-1}, so that in the end of the permeation run it becomes of the same order of magnitude as the recombination coefficients on the outlet side $K_2 = (0.6–5) \times 10^{-25}$ H^{-1} cm^4 s^{-1}.

The absorption coefficients have also been obtained from the experiment. Depending on the experimental conditions they cover a broad range of values $K_a = (3–200) \times 10^{12}$ H cm^{-2} s^{-1} Pa^{-1}, which are very low as they give a very low probability of absorption $A = (5–500) \times 10^{-7}$.

The conclusion has been made that permeation experiments with metals of the group V need special measures for purification of the hydrogen gas used.

References

[1] A.I. Livshits, M.E. Notkin, Yu.M. Pustovoit, A.A. Samartsev, Vacuum 29 (1979) 113.
[2] I. Ali-Khan, K.J. Dietz, F.G. Waelbroeck, P. Wienhold, J. Nucl. Mater. 76&77 (1978) 337.

[3] F. Waelbroeck, P. Wienhold, J. Winter, E. Rota, T. Banno, Influence of bulk and surface phenomena on the hydrogen permeation through metals, KFA Jülich, Report Jül-1966, 1984.
[4] K. Kizu, A. Pisarev, T. Tanabe, J. Nucl. Mater. 298 (2001) 291.
[5] A.I. Livshits, M.E. Notkin, A.A. Samartsev, J. Nucl. Mater. 170 (1990) 79.
[6] M. Yamawaki, N. Chitose, V. Bandurko, K. Yamaguchi, Fus. Eng. Design 28 (1995) 125.
[7] V. Bandurko, K. Yamaguchi, M. Yamawaki, T. Nagasaki, J. Nucl. Mater. 220–222 (1995) 904.
[8] W.M. Shu, Y. Hayashi, K. Okuno, J. Nucl. Mater. 220–222 (1995) 497.
[9] A.I. Livshits, M.E. Notkin, A.A. Samartsev, M.N. Solovyov, J. Nucl. Mater. 233–237 (1996) 1113.
[10] V. Bandourko, M. Yamawaki, K. Yamaguchi, V. Kurnaev, D. Levchuk, A. Pisarev, J. Nucl. Mater. 233–237 (1996) 1184.
[11] M. Takizawa, K. Kiuchi, M. Okamoto, Y. Fujii, J. Nucl. Mater. 248 (1997) 15.
[12] K. Ohkoshi, V. Alimov, K. Yamaguchi, M. Yamawaki, A.I. Livshits, J. Nucl. Mater. 266–269 (1999) 1167.
[13] G. Alefeld, J. Völkl (Eds.), Hydrogen in Metals, vols. I&II, Springer-Verlag, Berlin, 1978.
[14] S. Yamanaka, Y. Fujita, M. Uno, M. Katsuto, J. Alloys Compd. 293–295 (1999) 42.